Environmental Science & Technology

Subscriber access provided by NEW YORK MED COLL

Article

Macroscopic and spectroscopic assessment of the co-sorption of Fe(II) with As(III) and As(V) on Al-oxide

Ying Zhu, and Evert J. Elzinga

Environ. Sci. Technol., **Just Accepted Manuscript** • DOI: 10.1021/acs.est.5b04525 • Publication Date (Web): 27 Oct 2015

Downloaded from http://pubs.acs.org on October 31, 2015

Just Accepted

"Just Accepted" manuscripts have been peer-reviewed and accepted for publication. They are posted online prior to technical editing, formatting for publication and author proofing. The American Chemical Society provides "Just Accepted" as a free service to the research community to expedite the dissemination of scientific material as soon as possible after acceptance. "Just Accepted" manuscripts appear in full in PDF format accompanied by an HTML abstract. "Just Accepted" manuscripts have been fully peer reviewed, but should not be considered the official version of record. They are accessible to all readers and citable by the Digital Object Identifier (DOI®). "Just Accepted" is an optional service offered to authors. Therefore, the "Just Accepted" Web site may not include all articles that will be published in the journal. After a manuscript is technically edited and formatted, it will be removed from the "Just Accepted" Web site and published as an ASAP article. Note that technical editing may introduce minor changes to the manuscript text and/or graphics which could affect content, and all legal disclaimers and ethical guidelines that apply to the journal pertain. ACS cannot be held responsible for errors or consequences arising from the use of information contained in these "Just Accepted" manuscripts.

ACS Publications

Environmental Science & Technology is published by the American Chemical Society. 1155 Sixteenth Street N.W., Washington, DC 20036

Published by American Chemical Society. Copyright © American Chemical Society. However, no copyright claim is made to original U.S. Government works, or works produced by employees of any Commonwealth realm Crown government in the course of their duties.

Macroscopic and spectroscopic assessment of the co-sorption of Fe(II) with As(III) and As(V) on Al-oxide

Ying Zhu[1] and Evert J. Elzinga[1*]

[1] Rutgers University

Department of Earth & Environmental Sciences

101 Warren Street

Newark, NJ 07102, USA

*Corresponding author. Email: elzinga@rutgers.edu; phone: (+001)-973-353-5238

ABSTRACT

The co-sorption of Fe(II) with As(III) and As(V) in anoxic suspensions of γ-Al_2O_3 at pH 7.5 was investigated with batch kinetic experiments and synchrotron EXAFS analyses. Single-sorbate results showed that Fe(II) formed secondary Fe(II)-Al(III)-layered double hydroxide (LDH) phases during reaction with the Al-oxide sorbent, whereas As(III) and As(V) formed inner-sphere surface complexes. The kinetics and mechanisms of Fe(II) and As(III) sorption were identical in dual-sorbate and single-sorbate experiments, indicating that the processes involved operate independently. In contrast, As(V) and Fe(II) interacted strongly during co-sorption. Fe(II) enhanced the rate and extent of As(V) removal from solution, but did not affect the mechanism of As(V) adsorption. Conversely, As(V) hindered the formation of Fe(II)-Al(III)-LDH, slowing down precipitation at low As(V) concentrations and preventing it at high concentrations. This was attributed to interference of adsorbed As(V) with the Al supply needed for Fe(II)-Al(III)-LDH precipitation, possibly combined with enhanced surface complexation of Fe(II) cations promoted by anionic As(V) surface species. No evidence was found for redox reactions between Fe(II) and As(V) or As(III), or precipitation of Fe-arsenic phases. These results improve our understanding of the geochemistry of Fe(II) and arsenic in reducing environments, and demonstrate the utility of mechanistic studies on geochemically complex model systems.

INTRODUCTION

Sorption reactions at mineral-water interfaces have a profound impact on the solid-water partitioning of trace metal(loid)s and thus play an important role in controlling the mobility and fate of these species in soils and sediments.[1] Various studies have shown the ability of Al-bearing mineral substrates to induce the precipitation of Me(II)-Al(III)-layered double hydroxides (LDHs) during sorption of Ni(II), Zn(II) and Co(II) at near neutral pH values.[2–15] Our recent work has demonstrated that aqueous Fe(II) also readily precipitates during interaction with mineral sorbents, forming Fe(II)-Al(III)-LDH phases and poorly crystalline Fe(II)-phyllosilicates during sorption in anoxic suspensions of Al-oxide, smectite clay, and amorphous silica at pH values > 7.[16,17] The formation of such secondary Fe(II) phases may play an important role in determining Fe(II) sequestration and speciation in environments undergoing Fe(III) reduction, where concentrations of aqueous Fe(II) are elevated and pH values commonly are in the range 6.5-8.0.[18-24]

Reductive dissolution of Fe(III)-oxides not only leads to the build-up of high levels of aqueous Fe(II), but also releases trace metals and metalloids originally associated with these mineral sorbents.[18,20,24–26] The presence of dissolved trace metal(loid)s may affect the formation of secondary Fe(II) phases during Fe(II) sorption, while, conversely, the formation of Fe(II) precipitates may influence the retention of the aqueous metal(loid) species, e.g. through co-precipitation, adsorption or redox reactions. Therefore, studies of the co-sorption of Fe(II) with common trace elements are needed to obtain a better understanding of the formation of secondary Fe(II) precipitates and their impacts on trace metal(loid) solubility and speciation in suboxic and anoxic environments.

The current study focuses on the co-sorption of Fe(II) with the arsenic species arsenite, As(III) and arsenate, As(V), which are the dominant inorganic As species in groundwaters and soils,[27] using a model Al-oxide as the mineral sorbent. Previous studies have demonstrated that both As(III) and As(V) are sorbed effectively on Al-oxide substrates, but that the sorption affinities and mechanisms differ between the two As redox states. Arsenate adsorbs more extensively on Al-oxide than does arsenite under equivalent conditions, and spectroscopic work has shown that As(V) predominantly forms inner-sphere complexes at the Al-oxide surface whereas As(III) forms a mixture of outer- and inner-sphere complexes.[28–31] These differences in adsorption behavior may influence the impacts of these As species on the interaction of aqueous Fe(II) with Al-oxide sorbents.

Besides influencing the process of Fe(II)-Al(III)-LDH precipitation, the presence of arsenate and arsenite oxyanions may also affect the complexation of Fe(II) cations at the Al-oxide surface (i.e. Fe(II) adsorption). Results from past studies have indicated the potential of oxyanion co-sorbates for modifying metal adsorption through surface electrostatic effects and ternary complex formation.[32–39] Additional processes of potential importance include the precipitation of secondary Fe(II)-arsenic phases, and redox reactions between sorbed Fe(II) and As. Clearly, the geochemical complexity of dual-sorbate Fe(II)-As systems is substantially higher than those of the corresponding single-sorbate systems.

The objective of this study was to investigate the macroscopic and mechanistic aspects of the co-sorption of Fe(II) with As(III) and As(V) onto Al-oxide under anoxic conditions at pH 7.5. The experiments were conducted at conditions conducive to the formation of Fe(II)-Al(III)-LDH in order to assess the impacts of As(III) and As(V) on the precipitation process, and to determine the influence of these secondary Fe(II) phases on As retention. Our results demonstrate notable

differences in Fe(II) and arsenic sorption trends and mechanisms between single- and dual-sorbate systems, thus highlighting the need for mechanistic studies of model systems mimicking the complexity of natural environments.

EXPERIMENTAL SECTION

Experimental conditions and materials

All experiments were conducted under strictly anoxic conditions using a glovebox filled with 95% $N_{2(g)}$ and 5% $H_{2(g)}$, and equipped with Pd catalyst to scrub the atmosphere off trace $O_{2(g)}$. The anoxic protocols employed here are described in detail in our previous studies.[16, 17] An anoxic stock solution of 1.0 M Fe(II) was prepared by dissolving $FeCl_2 \cdot 4H_2O$ (Fisher Scientific, Cat. No. I90-500) in anoxic 0.1 M HCl and filtering the resulting solute through a 0.22 μm nitrocellulose membrane. Anoxic As(III) and As(V) stock solutions of 0.1 M were prepared from $NaAsO_2$ (Fisher Scientific, Cat. No. S225I-100) and $Na_2HAsO_4 \cdot 7H_2O$ (Sigma-Aldrich, Cat. No. 455857) salts, respectively. The mineral sorbent used in this study was γ-Al_2O_3 (Alfa Aesar, Cat. No. 39812), with a specific surface area measured as 70.5 $m^2\ g^{-1}$ using the N_2-BET method.

Batch sorption studies

Sorption experiments were conducted with anoxic 5.0 g γ-Al_2O_3 L^{-1} suspensions maintained at pH 7.5 with 50 mM HEPES dissolved in the electrolyte background. The ionic strength was set at 0.1 M with NaCl after accounting for the buffer speciation and the addition of titrant NaOH.

Kinetic experiments were performed in a total of 9 batches comprised of 5 single-sorbate and 4 dual-sorbate systems. For the single-sorbate experiments, γ-Al_2O_3 suspensions were spiked with either Fe(II) (1 mM), As(III) (0.25 mM) or As(V) (0.10 mM, 0.25 mM or 0.50 mM). In the

dual-sorbate systems, Fe(II) (1 mM) was added to the γ-Al_2O_3 suspensions simultaneously with either As(III) or As(V) at the same concentrations as used for the single-sorbate experiments. Aqueous speciation calculations using Mineql+[40] showed that the speciation of aqueous Fe(II) is dominated by non-complexed $Fe^{2+}_{(aq)}$ (97.8 %) with a minor component of $FeCl^{+}_{(aq)}$ (2.2 %), whereas aqueous As(III) consists of 97.9 % $H_3AsO_3^{0}{}_{(aq)}$ and 2.1 % $H_2AsO_3^{-}{}_{(aq)}$, and aqueous As(V) consists of 88.2 % $HAsO_4^{2-}{}_{(aq)}$ and 11.8 % $H_2AsO_4^{-}{}_{(aq)}$.

The reaction vessels were wrapped in aluminum foil to prevent light exposure, and sealed in three zip-lock bags inside the glovebox to prevent accidental exposure to O_2 during equilibration. The containers were sampled regularly over the course of 9 months to monitor the sorption of Fe(II), As(III) and As(V). Sampling involved retrieval of a 5 mL suspension aliquot which was filtered through a 0.22 μm nitrocellulose membrane inside the glovebox. The filtrates were acidified with 125 μL of 37 % HCl, and analyzed for the concentration of dissolved Fe(II) with the ferrozine method,[41] and/or for the concentration of aqueous arsenic using ICP-OES. Ion sorption was calculated as the difference between the initial and final solution concentrations.

Speciation calculations using the solubility product (K_{sp}) of symplesite ($Fe^{II}_3(As^{V}O_4)_2{\cdot}8H_2O$) reported by Johnston and Singer[42] indicated that the initial solutions of the dual-sorbate experiments with As(V) were oversaturated with respect to this phase. The saturation state of the equilibrated solutions, however, could not be assessed, because the aqueous As(V) concentrations were below the detection limit of ICP-OES. Catalano et al.[43] showed that the K_{sp} value used in the thermodynamic calculations may under-predict symplesite solubility in dilute solutes such as used here. We therefore experimentally assessed the potential of Fe(II)-As(V) precipitation in our systems, in two ways. First, we prepared blank samples that lacked γ-Al_2O_3 but were otherwise identical to the ternary sorption examples. The solutions were

filtered through 0.22 μm nitrocellulose membranes and analyzed. No removal of aqueous Fe(II) or As(V) was observed. Secondly, the XAS data of the sorption samples were compared to those of a synthetic Fe(II)-As(V) precipitate (details in the next section), and to those of symplesite as reported in Jönsson and Sherman.[44] These comparisons showed no evidence for Fe(II)-As(V) precipitation as discussed in the Results section below.

XAS studies

Samples for X-ray absorption spectroscopy (XAS) analysis were prepared under the same conditions and with the same methods as for the kinetic experiments described above, using sample volumes of 50 mL to obtain enough paste for XAS analysis. Both single-sorbate and dual-sorbate samples were prepared, at equilibration times varying from 1 day to 9 months. The anoxic protocols used for XAS sample preparation and transport were described previously.[17]

Besides the sorption samples, the following reference compounds were analyzed as well: (1) aqueous Fe(II); (2) nikischerite ($NaFe^{II}_6Al_3(SO_4)_2(OH)_{18}(H_2O)_{12}$); (3) aqueous As(III); (4) aqueous As(V); and (5) a synthetic Fe(II)-As(V) precipitate. The $Fe(II)_{(aq)}$ and nikischerite references are described in Zhu and Elzinga,[16] while the aqueous As(III) and As(V) standards were prepared as solutions of 10 mM $NaAsO_2$ and $Na_2HAsO_4{\cdot}7H_2O$ dissolved in DDI water. The Fe(II)-As(V) precipitate was prepared per the protocol of symplesite synthesis of Jönsson and Sherman.[44] Powder X-ray diffraction analysis of the mineral product showed broad diffraction peaks indicative of a poorly crystalline solid (not shown). XAS analyses confirmed that the local coordination environments of Fe and As in the solid resembled those of symplesite, as described in more detail in the Supporting Information (SI).

Synchrotron Fe *K*-edge (7112 eV) and As *K*-edge (11,867 eV) spectra were recorded on beamline X-11A of the National Synchrotron Light Source at Brookhaven National Laboratory, and beamline 12-BMB of the Advanced Photon Source at Argonne National Laboratory. The data were collected at room temperature in fluorescence mode using a Si(111) monochromator detuned by 40 % for Fe scans and by 25 % for As scans to suppress higher order harmonics. Fe foil and Au foil (L_{III}-edge 11,919 eV) were used for energy calibration of the Fe and As K-edges, respectively. The possibility of beam damage of the Fe(II) sorption samples during analysis was checked by comparing the normalized spectra of the first and last scan of each sample, as in Elzinga[17]. No damage was observed. EXAFS data processing and fitting were performed with WINXAS 3.1,[45] combined with Feff 7.0 [46] and ARTEMIS.[47] Details of the EXAFS data fitting routines used for the sorption and reference samples are described in the SI.

RESULTS

Batch kinetic studies

Figure 1 compares the kinetics of sorption of Fe(II) (1 mM) in the absence and presence of As(III) (0.25 mM) and As(V) (0.10, 0.25 and 0.50 mM). Consistent with our earlier studies,[16, 17] the Fe(II) sorption kinetics in the single-sorbate experiment are biphasic, with fast uptake during the first hours of reaction followed by a slower sorption stage that continues until equilibrium is reached after ~30 days (Figure 1). Effects of arsenic depend on As oxidation state and concentration. The presence of 0.25 mM As(III) does not discernibly affect the kinetics and extent of Fe(II) sorption, indicating that As(III) has little impact on Fe(II) retention even at this relatively high concentration (Figure 1a). The presence of As(V), in contrast, noticeably changes the kinetics of Fe(II) sorption, although the extent of sorption is relatively unaffected with 75-85 %

of Fe(II) ultimately removed under all conditions (Figure 1b). The kinetic impacts of As(V) vary with concentration. At the two lower As(V) additions (0.10 mM and 0.25 mM), the Fe(II) sorption kinetics slow down relative to the binary Fe(II)/γ-Al_2O_3 system, with the time required to attain apparent equilibrium increasing to ~100 days in the presence of 0.10 mM As(V), and to ~240 days in the presence of 0.25 mM As(V). At the highest level of As(V) addition (0.50 mM), on the other hand, Fe(II) sorption reaches equilibrium on a similar time scale as for the binary system, stabilizing within the first month of reaction (Figure 1b).

Figure 2 compares the sorption kinetics of As(III) and As(V) in the presence and absence of Fe(II). The retention of As(III) is not influenced by Fe(II), as shown by the similarity of the As(III) kinetic sorption patterns in the binary As(III)/γ-Al_2O_3 and ternary As(III)/Fe(II)/γ-Al_2O_3 suspensions (Figure 2a). This finding resembles the results of Figure 1a showing that As(III) does not affect the sorption of Fe(II). Combined, these observations suggest that the processes controlling the removal of aqueous Fe(II) and As(III) in the ternary samples are neither competitive nor synergistic, but operate independently under the conditions investigated here.

Contrariwise, the presence of Fe(II) enhances both the rate and extent of As(V) sorption relative to the binary As(V)/γ-Al_2O_3 systems, mediating rapid and essentially complete removal of As(V) from solution (Figure 2b-d). This promotive effect of Fe(II) on the sorption of As(V) contrasts with the inhibitive effect of As(V) on the sorption of Fe(II) at [As(V)]=0.10 and 0.25 mM (Figure 1b). These opposite impacts of co-sorption demonstrate the complexity of ternary sorption systems, where interactions between multiple processes complicate prediction of net outcomes.[32-39] Overall, the kinetic data presented in Figures 1 and 2 indicate that the arsenic oxidation state and concentration are important factors in regulating As impacts on Fe(II) sorption behavior on Al-oxide, and that the influence of Fe(II) on the sorption of arsenic depends

188 on the As oxidation state. The mechanisms behind these macroscopic sorption trends are
189 addressed below based on EXAFS spectroscopic results.
190
191 **Fe *K*-edge EXAFS data**
192 Figure 3 presents the Fe K-edge EXAFS data of the binary and ternary Fe(II) sorption samples
193 and Fe reference compounds, with Figure 3a showing the raw and fitted k^3-weighted χ spectra,
194 and Figure 3b the corresponding radial structure functions (RSFs) obtained from Fourier
195 transforming the raw χ data. The fit results are summarized in Table S1.
196 The Fe EXAFS spectra of the sorption samples vary with reaction time, As oxidation
197 state, and As concentration (Figure 3), indicating that these variables influence the speciation of
198 sorbed Fe. The Fourier transforms of all samples exhibit a peak at ~1.6 Å (uncorrected for phase
199 shift), which is due to backscattering from first-shell O ligands. This shell is fitted with 4.8-6.0 O
200 atoms at a radial distance of 2.08-2.12 Å (Table S1). These results indicate that sorbed Fe is
201 present in the divalent form and in octahedral coordination with first-shell O, as in the reference
202 compounds Fe(II)(aq) and nikischerite.[16, 17, 48–50] The persistence of Fe(II) as the predominant Fe
203 species in the ternary systems indicates that redox reactions between Fe(II) and As(V) or As(III)
204 co-sorbates do not occur to a significant extent.
205 The RSFs of the binary Fe(II)/γ-Al_2O_3 sorption samples exhibit a second shell at ~2.8 Å
206 (uncorrected for phase shift) (Figure 3b), which is due to backscattering from second-neighbor
207 Fe/Al and thus indicates the formation of Fe(II) precipitates. The k^3-weighted χ spectra (Figure
208 3a) and fit results (Table S1) of these samples closely resemble those of the nikischerite
209 reference (Figure 3a), identifying the precipitate formed as a Fe(II)-Al(III)-layered double
210 hydroxide (LDH). These findings are consistent with our previous studies showing Fe(II)-

Al(III)-LDH as the main Fe(II) sorption product of the interaction of Fe(II) with Al-oxide and clay substrates under similar conditions as used here.[16, 17] These Fe(II) phases consist of brucitic $Fe(OH)_2$ layers in which 1/3 of Fe(II) has been substituted with Al(III), generating a positive structural layer charge that is neutralized by interlayer Cl^- anions derived from the background electrolyte.[17, 48] In line with our previous results,[16, 17] precipitation of Fe(II)-Al(III)-LDH occurs rapidly in the binary experiments, with clear evidence for the presence of these phases after 2 h (Figure 3, spectrum b).

The Fe EXAFS results of the ternary samples show that Fe(II)-Al(III)-LDH precipitation occurs in the presence of As as well (Figure 3), but that the rate and extent of precipitation are modified in dependence of the As oxidation state and concentration. In the system containing As(III), precipitation of Fe(II)-Al(III)-LDH occurs on a similar time scale as in the binary Fe(II)/γ-Al_2O_3 system, with Fe(II)-Al(III)-LDH observed after 1 day (Figure 3 spectrum d). The apparent lack of interference of As(III) with the precipitation of Fe(II)-Al(III)-LDH is consistent with the macroscopic data of Figures 1a and 2a which similarly suggest that the sorption of Fe(II) and As(III) are mutually independent under the current experimental conditions.

In contrast to As(III), the presence of As(V) interferes with the precipitation of Fe(II)-Al(III)-LDH. This is demonstrated by spectra f-p in Figure 3, which were collected for the 1 d, 6 d, 35 d, and 8-9 mo samples of the ternary samples containing 0.10, 0.25 and 0.50 mM As(V). These data show that after 1 day of reaction, none of the ternary samples contain Fe(II)-Al(III)-LDH (Figure 3, spectra f, i, m). This contrasts with the As(V)-free Fe(II)/γ-Al_2O_3 system where formation of Fe(II)-Al(III)-LDH occurs within 2 hours (Figure 3, spectrum b). Precipitation of Fe(II)-Al(III)-LDH does ultimately occur as well in the ternary samples with 0.10 and 0.25 mM As(V), with evidence for the presence of these phases visible after 6 d and 35 d, respectively

(Figure 3). In the ternary system containing 0.50 mM As(V), however, there is no evidence for precipitation of Fe(II)-Al(III)-LDH even after 8 months of reaction (Figure 3, spectrum p; Table S1). Use of the Fe EXAFS results for identification of the mode of Fe(II) sorption in this system is limited by the lack of well-defined scattering contributions from atomic neighbors beyond first-shell O (Figure 3b, spectra m-p). We do, however, note the dissimilarity of the Fe XAS data of this system to those of the reference Fe(II)-As(V) precipitate (spectrum r in Figure 3), and those of crystalline symplesite reported by Jönsson and Sherman.[44] This suggests that formation of secondary Fe(II)-As(V) phases is not a major process. Constraints on the mechanisms of Fe(II) retention in this system are discussed below based on the combined Fe and As EXAFS spectroscopic data and the macroscopic sorption trends.

As *K*-edge EXAFS data

The As EXAFS data of sorption samples and reference compounds are displayed in Figure 4, and the fit results are presented in Table S2. Only the 6-day sorption samples are shown, because no changes were observed in the As XAS data over the course of the experiment (Figure S4-S7). The k^3-weighted χ spectra are dominated by the sinusoidal oscillations resulting from the backscattering of first-shell O neighbors (Figure 4a). The radial distance of first-shell O is fitted at 1.68 Å for the As(V) samples, and at 1.78-1.79 Å for the As(III) samples (Table S2), which are values consistent with the As(III)-O and As(V)-O coordination observed in previous XAS studies.[e.g. 28, 39, 43, 44, 51-54] There are no differences in the As(III)-O and As(V)-O coordination of the ternary and binary samples (Table S2). This indicates that the valence states of these arsenic species do not change during co-sorption with Fe(II), an observation that is consistent with the

Fe EXAFS results which similarly demonstrated the absence of redox reactions between Fe(II) and As(III) or As(V) (Figure 3; Table S1).

The RSFs of the As(III) and As(V) sorption samples (Figure 4b) show a second coordination shell at ~3.0 Å (uncorrected for phase shift). This shell was fitted with Al atomic neighbors located at a radial distance of 3.13-3.15 Å for the As(V) samples, and 3.22-3.25 Å for the As(III) samples (Table S2). These results are consistent with previous XAS studies of As(III) and As(V) adsorption on Al-oxide substrates,[e.g. 28, 39, 51, 54] and indicate the formation of inner-sphere bidentate binuclear complexes for both As(III) and As(V) at the γ-Al_2O_3 surface.

We note the strong similarity of the As(III) and As(V) XAS spectra and fit results obtained for the binary (i.e. As(III)/γ-Al_2O_3 and As(V)/γ-Al_2O_3) and the corresponding ternary sorption samples (Figures 4 and S9; Table S2). This indicates that any differences in the As(III) and As(V) speciation between the binary and ternary systems are minor. This is particularly noteworthy for the As(V) systems, where effects of Fe(II) on As sorption are strong (Figure 2), and therefore mechanistic differences in As(V) retention between binary and ternary samples might be expected. We note that the As(V) XAS data of the ternary systems do not resemble those of the reference Fe(II)-As(V) precipitate (spectrum e in Figure 4), and that the data fits are inconsistent with precipitation of symplesite (Table S2). Instead, the As(V) XAS data of the binary As(V)/γ-Al_2O_3 and ternary Fe(II)/As(V)/γ-Al_2O_3 systems are essentially identical (Figure 4; Table S2), as illustrated particularly well by the overlay of the As(V) χ spectra presented in Figure S9d. These results indicate that Fe(II) has no noticeable impact on the mode of As retention in our experimental systems, with As(III) and As(V) adsorbed as inner-sphere bidentate binuclear complexes at the Al-oxide surface in both the presence and absence of Fe(II).

DISCUSSION

Mechanisms of Fe(II) and As(III) co-sorption

The combined macroscopic and spectroscopic data presented here suggest that As(III) and Fe(II) react independently with the γ-Al_2O_3 substrate, as indicated by the identical results obtained for the ternary and binary sorption systems in terms of the rate, extent and mechanisms of Fe(II) and As(III) sorption (Figures 1-4; Tables S1 and S2). The XAS results demonstrate that As(III) coordinates as inner-sphere adsorption complexes at the γ-Al_2O_3 surface, while Fe(II) forms secondary Fe(II)-Al(III)-LDH precipitates with Al(III) supplied by partial dissolution of the Al-oxide sorbent.

The absence of a discernable effect of Fe(II) on the adsorption of As(III) at the γ-Al_2O_3 surface indicates that the secondary Fe(II)-Al(III)-LDH precipitates formed in the ternary samples do not represent a significant sink for As(III) compared to the γ-Al_2O_3 surface. This is likely at least in part due to the relatively small amount of Fe(II) (1.0 mM) in the system compared to Al (98 mM), limiting the potential of Fe(II)-Al(III)-LDH to act as a quantitatively important sorbent relative to the γ-Al_2O_3 substrate. An additional consideration is that Fe(II)-Al(III)-LDH may not have a particularly high affinity for sorption of As(III). The surface of Fe(II)-Al(III)-LDH is dominated by positively charged basal surfaces,[17, 48] whereas the dominant aqueous As(III) species in our experimental systems is charge-neutral $H_3AsO_3^0{}_{(aq)}$. The absence of favorable electrostatic interactions between $H_3AsO_3^0{}_{(aq)}$ and Fe(II)-Al(III)-LDH may limit the adsorption of aqueous As(III) onto this secondary Fe(II) phase, especially in the presence of the relatively high concentration of Cl^- anions provided by the 0.10 M NaCl background electrolyte. Studies addressing the affinity and mechanisms of As(III) interaction with Fe(II)-Al(III)-LDH are needed to assess the potential of this Fe(II) mineral phase to act as a sink of As(III).

The dominant mode of Fe(II) sorption in the ternary Fe(II)/As(III)/γ-Al_2O_3 systems is the formation of Fe(II)-Al(III)-LDH phases (Figure 3). However, in view of the relatively high solution pH and the fact that some Fe(II) remains in solution (Figure 1), adsorption of Fe(II) to the γ-Al_2O_3 surface is expected to occur as well.[16, 17] Assuming that the resulting Fe(II) surface complexes are inner-sphere, as observed for the divalent metals Zn(II) and Pb(II),[55, 56] the Al-oxide surface charge is expected to increase (i.e. become more positive) in the presence of aqueous Fe(II). Since the adsorption of As(III) is not sensitive to this presumed change in the surface charge of the mineral sorbent (Figure 2a), we infer that the As(III) surface complexes are charge-neutral. This conclusion is consistent with the predominant occurrence of aqueous As(III) as the (uncharged) $As(OH)_3^0{}_{(aq)}$ species in our systems, and is supported by the electrophoretic mobility measurements of Arai et al.[28], who demonstrated that the surface charge of γ-Al_2O_3 is not modified by As(III) adsorption. Verification of this argument will require studies characterizing the mononuclear adsorption complexes formed by Fe(II) at the Al-oxide surface.

A final point we make from the Fe(II)-As(III) co-sorption results is that the As(III) surface complexes do not appear to affect the availability of sorbent-derived Al for formation of Fe(II)-Al(III)-LDH. We have previously proposed that the slow stage of Fe(II) sorption, which occurs between 1-30 days under the current conditions (Figure 1), is due to ongoing precipitation of Fe(II)-Al(III)-LDH, and is rate-controlled by the dissolution of the Al-oxide sorbent supplying the Al needed for LDH precipitation, consistent with the conclusions from other studies.[7, 16, 17, 56, 57] The identical kinetics of Fe(II) sorption in the absence and presence of As(III) (Figure 1a) therefore indicate that the release of Al from the surface is not affected by adsorbed As(III). This suggests that the interaction of As(III) with the Al-oxide surface is insufficiently strong to interfere with Al-oxide dissolution.

325

326 **Mechanisms of Fe(II) and As(V) co-sorption**

327 The experiments conducted with As(V) and Fe(II) demonstrate distinctly different
328 sorption behavior of both species in ternary versus binary systems, indicating interactions
329 between the two during co-sorption. The presence of Fe(II) strongly increases the sorption of
330 As(V) (Figure 2). However, the As XAS data indicate that the mode of As(V) retention is not
331 noticeably modified by the presence of Fe(II) (Figure 4, S9; Table S2). We therefore exclude
332 formation of Fe(II)-As(V) precipitates and sorption of As(V) onto secondary Fe(II)-Al(III)-LDH
333 phases as significant drivers of the observed enhancement of As(V) sorption in the presence of
334 Fe(II). Instead, the current results suggest surface electrostatic effects as a plausible cause for the
335 increase in As(V) sorption in the ternary experiments. In this scenario, the Al-oxide surface
336 becomes more positively charged due to inner-sphere complexation of Fe(II) cations, and this
337 promotes additional sorption of anionic As(V) (relative to the binary As(V)/γ-Al_2O_3 system) by
338 lowering the electrostatic barrier for ion approach. The dominant aqueous As(V) in our
339 experimental systems is anionic $HAsO_4^{2-}{}_{(aq)}$, and the electrophoretic mobility studies of Arai et
340 al.[28] indicate that the inner-sphere adsorption complexes of As(V) at the Al-oxide surface carry
341 negative charge. The electrostatics of the As(V)/γ-Al_2O_3 surface interaction thus favor increased
342 As(V) adsorption mediated by inner-sphere surface complexation of Fe(II). As noted above, the
343 inner-sphere coordination of Fe(II) cations and the consequent increase in Al-oxide surface
344 charge remains to be confirmed, but is consistent with the mechanisms of Zn(II) and Pb(II)
345 adsorption onto γ-Al_2O_3.[13, 55]

346 Besides electrostatic effects, direct interactions between adsorbed Fe(II) and As(V)
347 surface complexes may occur as well. Such interactions lead to the formation of ternary surface

complexes exhibiting chemical or physical bonds between adsorbed Fe(II) and As(V) that increase the stability of sorption of both species. Ternary complexes have been observed in IR studies of the co-sorption of oxyanions like phosphate, sulfate and carbonate with various divalent metals (including Fe(II)) on Fe(III)-oxide substrates,[32-39, 58, 59] and have been suggested to occur during co-sorption of Co(II) and Se(IV) (as the selenite oxyanion SeO_3^{2-}) onto γ-Al_2O_3.[60, 61] If similar As(V)-Fe(II) ternary surface complexes are formed to a significant extent in our systems, they do not induce a major change in the interaction of As(V) with the Al-oxide surface, as shown by the As EXAFS data (Figure 4; Table S2). This suggests that they are either ligand-bridged (i.e. arranged as γAl_2O_3-As(V)-Fe(II)) or involve lateral interactions between adsorbed Fe(II) and As(V). Unfortunately, EXAFS spectroscopy is relatively insensitive towards detection of small numbers of second-neighbor atomic scatterers, especially if the coordination is relatively disordered, making identification and characterization of ternary surface complexes difficult with this technique.[32] Application of IR measurements would be useful in resolving the potential importance of ternary complexes in these systems.

The sorption of Fe(II) is slower in the ternary experiments with the two lower As(V) (0.10 and 0.25 mM) than in the binary Fe(II)/γ-Al_2O_3 experiment (Figure 1b), although the main mode of Fe(II) retention in the ternary systems remains the precipitation of Fe(II)-Al(III)-LDH (Figure 3). The Fe EXAFS data demonstrate that As(V) noticeably slows down the formation of secondary Fe(II)-Al(III)-LDH (Figure 3; Table S1), explaining the slower rate of Fe(II) sorption observed macroscopically. These results resemble those of Boyle-Wright et al.[61], who similarly observed that the precipitation of Co(II)-Al(III)-LDH during Co(II) interaction with γ-Al_2O_3 is hindered by the presence of Se(IV), a strongly sorbing oxyanion, as a co-sorbate. The inhibitive effect of As(V) on LDH precipitation may result from: (i) interaction of As(V) with growing

Fe(II)-Al(III)-LDH crystallites slowing down their growth; or (ii) interference of As(V) with the release of Al from the Al-oxide sorbent limiting the supply of Al available for Fe(II)-Al(III)-LDH precipitation. The As EXAFS data (Figure 4; Table S2) show no evidence for interaction of As(V) with Fe(II)-Al(III)-LDH in the ternary samples, but instead suggest that As(V) predominantly forms inner-sphere adsorption complexes at the Al-oxide surface. We therefore deem interference of As(V) with the Al supply required for precipitation of Fe(II)-Al(III)-LDH phases the more likely cause of their relatively slow growth in the ternary samples.

The presence of As(V) may inhibit the release of Al from the Al-oxide sorbent through two main mechanisms: (i) by blocking surface sites where Al release occurs through formation of inner-sphere surface complexes; and/or (ii) by forming As(V)-Al(III) precipitates that compete with the precipitation of Fe(II)-Al(III)-LDH phases as a sink of Al. The mechanism of surface site blocking has been demonstrated in studies with ferrihydrite, a metastable Fe(III)-oxide mineral, where the presence of adsorbed As(V) inhibited mineralogical transformation by inhibiting dissolution and re-precipitation of Fe(III).[e.g.62-65] Boyle-Wight et al.[61] suggested scavenging of Al(III) through formation of Se(IV)-Al(III) inner-sphere complexes or precipitates as a likely cause of the inhibitive effect of Se(IV) on Co(II)-Al(III)-LDH precipitation in Co(II)/Se(IV)/γ-Al_2O_3 sorption experiments. D'Espinose de la Caillerie et al.[66] observed that γ-Al_2O_3 dissolution was promoted by reaction with Ni(II) and Co(II) at pH 7.0-8.2 forming Ni(II)- and Co(II)-Al(III)-LDH precipitates, and suggested that adsorbed divalent metal cations may weaken structural Al-O bonds thereby accelerating the dissolution of the γ-Al_2O_3 sorbent. Based on this argument, blocking of surface sites by As(V) may reduce the extent of Fe(II) surface complexation and thereby the rate of Al release and Fe(II)-Al(III)-LDH formation. Precipitation of As(V)-Al(III) phases was proposed by Arai and Sparks[28] as an explanation for the increased

resistance of As(V) to desorption during long-term aging in γ-Al_2O_3 suspensions. Our As EXAFS data show no discernable change in As(V) speciation over the duration of the experiments (Figures 4 and S4-S7; Table S2), implying that any arsenate-aluminum phases formed either are present at concentrations too low to be detected by bulk EXAFS, or have an As-Al coordination similar to that of the inner-sphere As(V) adsorption complexes on the Al-oxide surface. Resolving the mechanism of As(V) interference with Al release will require detailed additional characterization of the As(V) interaction with Al-oxide substrates, particularly with respect to the potential role of As(V)-Al(III) precipitates as a long-term sink of As(V).

Fe(II)-Al(III)-LDH phases do not form in the ternary experiment with the highest level of As(V) co-addition (0.5 mM; Figure 3). The Fe speciation in this system is otherwise, however, poorly constrained by the Fe EXAFS results because of the absence of well-defined scattering from second-shell atomic neighbors (Figure 3b). The data do not resemble that of the reference Fe(II)-As(V) precipitate (Figure 3), which suggests that formation of such phases does not occur. This is corroborated by the As *K*-edge EXAFS data demonstrating that arsenate is dominantly adsorbed onto the γ-Al_2O_3 surface with no evidence to suggest precipitation with Fe(II) (Figure 4; S9d). From these results, we infer that Fe(II) most likely is present as mononuclear surface species, a conclusion that is consistent with the relatively fast Fe(II) sorption kinetics observed macroscopically (Figure 1b). The lack of distinct second-neighbor scattering points to a disordered average local coordination around adsorbed Fe(II), suggestive of the existence of multiple coordination environments. The concentration of Al surface sites in the system is estimated at 1.35 mM based on the specific surface area of the γ-Al_2O_3 sorbent (70.5 m^2 g^{-1}), the γ-Al_2O_3 suspension density (5.0 g L^{-1}) , and an assumed surface site density of 2.3 sites nm^{-2}.[67]

417 This concentration is similar to the sum of the concentrations of aqueous As(V) and Fe(II)
418 removed from solution in this ternary system, where 0.5 mM of aqueous As(V) is removed from
419 solution (Figure 2d) and ~0.75 mM of aqueous Fe(II) is sorbed (Figure 1b). This suggests a
420 crowded surface where ternary interactions between sorbate Fe(II) and As(V) are likely, and
421 polynuclear species may form. We speculate that adsorbed Fe(II) may be simultaneously
422 engaged in interactions with Al-oxide surface sites and in ternary interactions with sorbed As(V)
423 and/or Fe(II), resulting in a mixture of different surface species. The absence of Fe(II)-Al(III)-
424 LDH precipitation in this high [As(V)] system may be the combined result of the apparent
425 interference of As(V) with the Al supply needed for LDH formation (as discussed above), and
426 the favorable conditions established by adsorbed As(V) for Fe(II) surface complexation through
427 surface electrostatic changes and ternary interactions. Clearly, additional work is required to
428 determine the Fe(II) surface speciation in this ternary system in more detail. Despite this
429 uncertainty, the results unambiguously demonstrate that As(V) induces a major change in the
430 speciation of sorbed Fe(II) relative to the As(V)-free system and the ternary system with the two
431 lower As(V) additions. Such impacts need to be understood for accurate prediction of the
432 geochemical fate of aqueous Fe(II) and the importance of Fe(II) precipitation in suboxic and
433 anoxic geochemical environments.
434

435 **ENVIRONMENTAL IMPLICATIONS**

436 The results presented here demonstrate the potential importance of mutual interactions between
437 released Fe(II) and As(III) or As(V) in controlling the solubility and speciation of these species
438 in reducing environments. We show that Fe(II) promotes the adsorption of As(V) onto the Al-
439 oxide surface, while the retention of As(III) is unaffected by the presence of Fe(II). In turn, the

precipitation of secondary Fe(II)-Al(III)-LDH phases during Fe(II) sorption proceeds unaffected by the presence of As(III), but slows down at low levels of As(V), and shuts down in systems with high As(V) concentrations, where Fe(II) surface complexes are formed instead. The observed effects of As valence imply that impacts of co-sorption likely will be minimal in highly reducing environments such as deep groundwaters containing reduced As(III), whereas strong impacts are expected in suboxic systems such as riparian soils containing As(V). The mutual interactions (or lack thereof) between Fe(II) and arsenic sorbates characterized here are critical to the development of qualitative and quantitative models of the speciation and fate of these species in reducing environments. Our results suggest that other environmental factors including pH and the presence of phosphate and natural organic matter are likely to impact Fe(II) precipitation in suboxic environments. Due to the resemblance in chemical properties of arsenate and phosphate, phosphate may exert a similar influence on Fe(II) sorption as observed here for arsenate. Organic substances have a high affinity for Al complexation, and may limit Al availability for Fe(II)-Al(III)-LDH precipitation. Solution pH impacts the solubility of Fe(II)-Al(III)-LDH and Al-oxide, and affects the extent of As sorption with the Al-oxide surface, which may impact Al availability based on the current results. Additional work is needed to address these issues.

SUPPORTING INFORMATION AVAILABLE

(1) Description of the EXAFS data fitting routines; (2) Assessment of the Fe and As speciation in the reference Fe(II)-As(V) precipitate; (3) Full set of As XAS data collected for this study.

ACKNOWLEDGEMENTS

462 This work was supported by National Science Foundation grant EAR-1226581. We thank the
463 beamline scientists at 12-BMB (APS) and X11A (NSLS) for assistance with data collection, and
464 Daniel Giammar and three anonymous reviewers for helpful review comments.

465

466 **REFERENCES**

467 (1) Sparks, D. L. *Environmental Soil Chemistry*, 2nd ed.; Academic Press: Boston, MA,
468 U.S.A., 2002.

469 (2) Thompson, H. A.; Parks, G. A.; Brown, G. E. Dynamic interactions of dissolution, surface
470 adsorption, and precipitation in an aging cobalt(II)-clay-water system. *Geochim.*
471 *Cosmochim. Acta* **1999**, *63*, 1767–1779.

472 (3) Ford, R. G.; Sparks, D. L. The nature of Zn precipitates formed in the presence of
473 pyrophyllite. *Environ. Sci. Technol.* **2000**, *34*, 2479–2483.

474 (4) Scheckel, K. G.; Sparks, D. L. Kinetics of the formation and dissolution of Ni precipitates
475 in a gibbsite/amorphous silica mixture. *J. Colloid Interface Sci.* **2000**, *229*, 222–229.

476 (5) Scheinost, A. C.; Sparks, D. L. Formation of layered single- and double-metal hydroxide
477 precipitates at the mineral/water interface: a multiple-scattering XAFS analysis. *J. Colloid*
478 *Interface Sci.* **2000**, *223*, 167–178.

479 (6) Scheidegger, A. M.; Sparks, D. L. Kinetics of the formation and the dissolution of nickel
480 surface precipitates on pyrophyllite. *Chem. Geol.*, **1996**, *132*, 157–164.

481 (7) Scheidegger, A. M.; Strawn, D. G.; Lamble, G. M.; Sparks, D. L. The kinetics of mixed
482 Ni-Al hydroxide formation on clay and aluminum oxide minerals: A time-resolved XAFS
483 study. *Geochim. Cosmochim. Acta* **1998**, *62*, 2233–2245.

484 (8) Towle, S. N.; Bargar, J. R.; Brown, G. E.; Parks, G. A. Surface precipitation of Co(II) (aq)
485 on Al_2O_3. *J. Colloid Interface Sci.* **1997**, *187*, 62–82.

486 (9) Elzinga, E. J.; Sparks, D. L. Reaction condition effects on nickel sorption mechanisms in
487 illite–water suspensions. *Soil Sci. Soc. Am. J.* **2001**, *65*, 94–101.

488 (10) Peltier, E.; Allada, R.; Navrotsky, A.; Sparks, D. L. Nickel solubility and precipitation in
489 soils: a thermodynamic study. *Clays Clay Miner.* **2006**, *54*, 153–164.

490 (11) Roberts, D. R.; Scheidegger, A. M.; Sparks, D. L. Kinetics of mixed Ni-Al precipitate
491 formation on a soil clay fraction. *Environ. Sci. Technol.* **1999**, *33*, 3749–3754.

(12) Elzinga, E. J.; Sparks, D. L. Nickel sorption mechanisms in a pyrophyllite-montmorillonite mixture. *J. Colloid Interface Sci.* **1999**, *213*, 506–512.

(13) Roberts, D. R.; Ford, R. G.; Sparks, D. L. Kinetics and mechanisms of Zn complexation on metal oxides using EXAFS spectroscopy. *J. Colloid Interface Sci.* **2003**, *263*, 364–376.

(14) Trainor, T. P.; Brown, G. E.; Parks, G. A. Adsorption and precipitation of aqueous Zn(II) on alumina powders. *J. Colloid Interface Sci.* **2000**, *231*, 359–372.

(15) Scheidegger, A. M.; Lamble, G. M.; Sparks, D. L. Spectroscopic evidence for the formation of mixed-cation hydroxide phases upon metal sorption on clays and aluminum oxides. *J. Colloid Interface Sci.* **1997**, *186*, 118–128.

(16) Zhu, Y.; Elzinga, E. J. Formation of layered Fe(II)-hydroxides during Fe(II) sorption onto clay and metal-oxide substrates. *Environ. Sci. Technol.* **2014**, *48*, 4937–4945.

(17) Elzinga, E. J. Formation of layered Fe(II)-Al(III)-hydroxides during reaction of Fe(II) with aluminum oxide. *Environ. Sci. Technol.* **2012**, *46*, 4894–4901.

(18) Ponnamperuma, F. N. The chemistry of submerged soils. *Adv. Agron.* **1972**, *24*, 29–96.

(19) Hem, J. D. *Study and interpretation of the chemical characteristics of natural water*, 3rd ed.; United States Government Printing Office: Washington DC, 1985.

(20) Borch, T.; Kretzschmar, R.; Kappler, A.; Cappellen, P. Van; Ginder-Vogel, M.; Voegelin, A.; Campbell, K. Biogeochemical redox processes and their impact on contaminant dynamics. *Environ. Sci. Technol.* **2010**, *44*, 15–23.

(21) Weber, K. A.; Achenbach, L. A.; Coates, J. D. Microorganisms pumping iron: anaerobic microbial iron oxidation and reduction. *Nat. Rev. Microbiol.* **2006**, *4*, 752–764.

(22) Lovley, D. R.; Phillips, E. J. P. Organic matter mineralization with reduction of ferric iron in anaerobic sediments. *Appl. Environ. Microbiol.* **1986**, *51*, 683–689.

(23) Baedecker, M. J.; Cozzarelli, I. M. The determination and fate of unstable constituents of contaminated groundwater. In *Groundwater contamination and analysis at hazardous waste sites*; Lesage, S.; Jackson, R. E., Eds.; Marcel Dekker, Inc.: New York, 1992; pp. 425.

(24) Kirk, G. *The Biogeochemistry of Submerged Soils*; John Wiley & Sons, Ltd: Chichester, U.K., 2004; p 282.

(25) Gambrell, R. P. Trace and toxic metals in wetlands—a review. *J. Environ. Qual.* **1994**, *23*, 883–891.

(26) Weber, F. A.; Voegelin, A.; Kretzschmar, R. Multi-metal contaminant dynamics in temporarily flooded soil under sulfate limitation. *Geochim. Cosmochim. Acta* **2009**, *73*, 5513–5527.

(27) Smedley, P.L.; Kinniburgh, D.G. A review of the source, behaviour and distribution of arsenic in natural waters. *Appl. Geochem.* **2002**, *17*, 517-568.

(28) Arai, Y.; Elzinga, E. J.; Sparks, D. L. X-ray absorption spectroscopic investigation of arsenite and arsenate adsorption at the aluminum oxide-water interface. *J. Colloid Interface Sci.* **2001**, *235*, 80–88.

(29) Goldberg, S.; Johnston, C. T. Mechanisms of arsenic adsorption on amorphous oxides evaluated using macroscopic measurements, vibrational spectroscopy, and surface complexation modeling. *J. Colloid Interface Sci.* **2001**, *234*, 204–216.

(30) Goldberg, S. Competitive adsorption of arsenate and arsenite on oxides and clay minerals. *Soil Sci. Soc. Am. J.* **2002**, *66*, 413–421.

(31) Frankenberger, W. T. *Environmental chemistry of arsenic*; Marcel Dekker, Inc.: New York, 2002.

(32) Elzinga, E. J.; Kretzschmar, R. In situ ATR-FTIR spectroscopic analysis of the co-adsorption of orthophosphate and Cd(II) onto hematite. *Geochim. Cosmochim. Acta* **2013**, *117*, 53–64.

(33) Bargar, J. R.; Brown, G. E.; Parks, G. A. Surface complexation of Pb(II) at oxide-water interfaces: III . XAFS determination of Pb(II) and Pb(II)-chloro adsorption complexes on goethite and alumina. *Geochim. Cosmochim. Acta* **1998**, *62*, 193–207.

(34) Weesner, F. J.; Bleam, W. F. Binding characteristics of Pb^{2+} on anion-modified and pristine hydrous oxide surfaces studied by electrophoretic mobility and X-ray absorption spectroscopy. *J. Colloid Interface Sci.* **1998**, *205*, 380–389.

(35) Ostergren, J. D.; Trainor, T. P.; Bargar, J. R.; Brown, G. E.; Parks, G. A. Inorganic ligand effects on Pb(II) sorption to goethite (α-FeOOH) I. Carbonate. *J. Colloid Interface Sci.* **2000**, *225*, 466–482.

(36) Ostergren, J. D.; Brown, G. E.; Parks, G. A.; Persson, P. Inorganic ligand effects on Pb(II) sorption to goethite (α-FeOOH) II. Sulphate. *J. Colloid Interface Sci.* **2000**, *225*, 483–493.

(37) Elzinga, E. J.; Peak, D.; Sparks, D. L. Spectroscopic studies of Pb(II)-sulfate interactions at the goethite-water interface. *Geochim. Cosmochim. Acta* **2001**, *65*, 2219–2230.

(38) Zhang, G. Y.; Peak, D. Studies of Cd(II)-sulfate interactions at the goethite-water interface by ATR-FTIR spectroscopy. *Geochim. Cosmochim. Acta* **2007**, *71*, 2158–2169.

(39) Tang, Y.; McDonald, J.; Reeder, R. J. Enhanced uranium sorption on aluminum oxide pretreated with arsenate. Part II: Spectroscopic studies. *Environ. Sci. Technol.* **2009**, *43*, 4452–4458.

(40) Schecher, W.; McAvoy, D. *MINEQL+[4.6]*; Environmental Research Software: Hallowell, ME, U.S.A., 2003.

(41) Stookey, L. L. Ferrozine - a new spectrophotometric reagent for iron. *Anal. Chem.* **1970**, *42*, 779–781.

(42) Johnston, R. B.; Singer, P. C. Solubility of symplesite (ferrous arsenate): implications for reduced groundwaters and other geochemical environments. *Soil Sci. Soc. Am. J.* **2007**, *71*, 101–107.

(43) Catalano, J. G.; Luo, Y.; Otemuyiwa, B. Effect of aqueous Fe(II) on arsenate sorption on goethite and hematite. *Environ. Sci. Technol.* **2011**, *45*, 8826–8833.

(44) Jönsson, J.; Sherman, D. M. Sorption of As(III) and As(V) to siderite, green rust (fougerite) and magnetite: implications for arsenic release in anoxic groundwaters. *Chem. Geol.* **2008**, *255*, 173–181.

(45) Ressler, T. WinXAS : a new software package not only for the analysis of energy-dispersive XAS data. *J. Phys. IV France* **1997**, *7*, C2–C269.

(46) Ankudinov, A. L.; Rehr, J. J. Relativistic calculations of spin-dependent x-ray-absorption spectra. *Phys. Rev. B* **1997**, *56*, R1712–R1715.

(47) Ravel, B.; Newville, M. ATHENA, ARTEMIS, HEPHAESTUS: data analysis for X-ray absorption spectroscopy using IFEFFIT. *J. Synchrotron Radiat.* **2005**, *12*, 537–541.

(48) Huminicki, D. M. C.; Hawthorne, F. C. The crystal structure of nikischerite, $NaFe^{2+}_6Al_3(SO_4)_2(OH)_{18}(H_2O)_{12}$, a mineral of the shigaite group. *Can. Mineral.* **2003**, *41*, 79–82.

(49) Olszewski, W.; Szymański, K.; Zaleski, P.; Zając, D. A. X-ray absorption near edge structure and extended X-ray absorption fine structure analysis of Fe(II) aqueous and acetone solutions. *J. Phys. Chem. A* **2011**, *115*, 13420–13424.

(50) Parise, J. B.; Marshall, W. G.; Smith, R. I.; Lutz, H. D.; Möller, H. The nuclear and magnetic structure of " white rust "— Fe $(OH_{0.86}D_{0.14})_2$. *Am. Mineral.* **2000**, *85*, 189–193.

(51) Voegelin, A.; Weber, F-A.; Kretzschmar, R. Distribution and speciation of arsenic around roots in a contaminated riparian floodplain soil: Micro-XRF element mapping and EXAFS spectroscopy. *Geochim. Cosmochim. Acta* **2007**, *71*, 5804–5820.

588 (52) Manning, B. A.; Fendorf, S. E.; Bostick, B.; Suarez, D. L. Arsenic(III) oxidation and
589 arsenic(V) adsorption reactions on synthetic birnessite. *Environ. Sci. Technol.* **2002**, *36*,
590 976–981.

591 (53) Makris, K. C.; Sarkar, D.; Parsons, J. G.; Datta, R.; Gardea-Torresdey, J. L. X-ray
592 absorption spectroscopy as a tool investigating arsenic(III) and arsenic(V) sorption by an
593 aluminum-based drinking-water treatment residual. *J. Hazard. Mater.* **2009**, *171*, 980–986.

594 (54) Arai, Y.; Sparks, D. L. Residence time effects on arsenate surface speciation at the
595 aluminum oxide-water interface. *Soil Sci.* **2002**, *167*, 303–314.

596 (55) Strawn, D. G.; Scheidegger, A. M.; Sparks, D. L. Kinetics and mechanisms of Pb(II)
597 sorption and desorption at the aluminum oxide-water interface. *Environ. Sci. Technol.*
598 **1998**, *32*, 2596–2601.

599 (56) Li, W.; Livi, K. J. T.; Xu, W.; Siebecker, M. G.; Wang, Y.; Phillips, B. L.; Sparks, D. L.
600 Formation of crystalline Zn-Al layered double hydroxide precipitates on γ-alumina: the
601 role of mineral dissolution. *Environ. Sci. Technol.* **2012**, *46*, 11670–11677.

602 (57) Scheinost, A. C.; Ford, R. G.; Sparks, D. L. The role of Al in the formation of secondary
603 Ni precipitates on pyrophyllite, gibbsite, talc, and amorphous silica: A DRS study.
604 *Geochim. Cosmochim. Acta* **1999**, *63*, 3193–3203.

605 (58) Ali, M. A.; Dzombak, D. A. Interactions of copper, organic acids, and sulfate in goethite
606 suspensions. *Geochim. Cosmochim. Acta* **1996**, *60*, 5045–5053.

607 (59) Hinkle, M. A. G.; Wang, Z.; Giammar, D. E.; Catalano, J. G. Interaction of Fe(II) with
608 phosphate and sulfate on iron oxide surfaces. *Geochim. Cosmochim. Acta* **2015**, *158*, 130–
609 146.

610 (60) Boyle-Wight, E. J.; Katz, L. E.; Hayes, K. F. Macroscopic studies of the effects of
611 selenate and selenite on cobalt sorption to γ-Al_2O_3. *Environ. Sci. Technol.* **2002**, *36*, 1212–
612 1218.

613 (61) Boyle-Wight, E. J.; Katz, L. E.; Hayes, K. F. Spectroscopic studies of the effects of
614 selenate and selenite on cobalt sorption to γ-Al_2O_3. *Environ. Sci. Technol.* **2002**, *36*, 1219–
615 1225.

616 (62) Erbs, J. J.; Berquó, T. S.; Reinsch, B. C.; Lowry, G. V.; Banerjee, S. K.; Penn, R. L.
617 Reductive dissolution of arsenic-bearing ferrihydrite. *Geochim. Cosmochim. Acta* **2010**,
618 *74*, 3382–3395.

619 (63) Gomez, M. A.; Hendry, M. J.; Hossain, A.; Das, S.; Elouatik, S. Abiotic reduction of 2-
620 line ferrihydrite: effects on adsorbed arsenate, molybdate, and nickel. *RSC Adv.* **2013**, *3*,
621 25812–25822.

(64) Masue-Slowey, Y.; Loeppert, R. H.; Fendorf, S. Alteration of ferrihydrite reductive dissolution and transformation by adsorbed As and structural Al: Implications for As retention. *Geochim. Cosmochim. Acta* **2011**, *75*, 870–886.

(65) Manceau, A. The mechanism of anion adsorption on iron oxides: Evidence for the bonding of arsenate tetrahedra on free $Fe(O, OH)_6$ edges. *Geochim. Cosmochim. Acta* **1995**, *59*, 3647–3653.

(66) d'Espinose de la Caillerie, J-P.; Kermarec, M.; Clause, O. Impregnation of γ-alumina with Ni(II) or Co(II) ions at neutral pH: Hydrotalcite-type coprecipitate formation and characterization. *J. Am. Chem. Soc.* **1995**, *117*, 11471-11481.

(67) Davis, J. A.; Kent, D. B. Surface complexation modeling in aqueous geochemistry *Rev. Mineral. Geochem.* **1990**, 23, 177– 260.

FIGURES

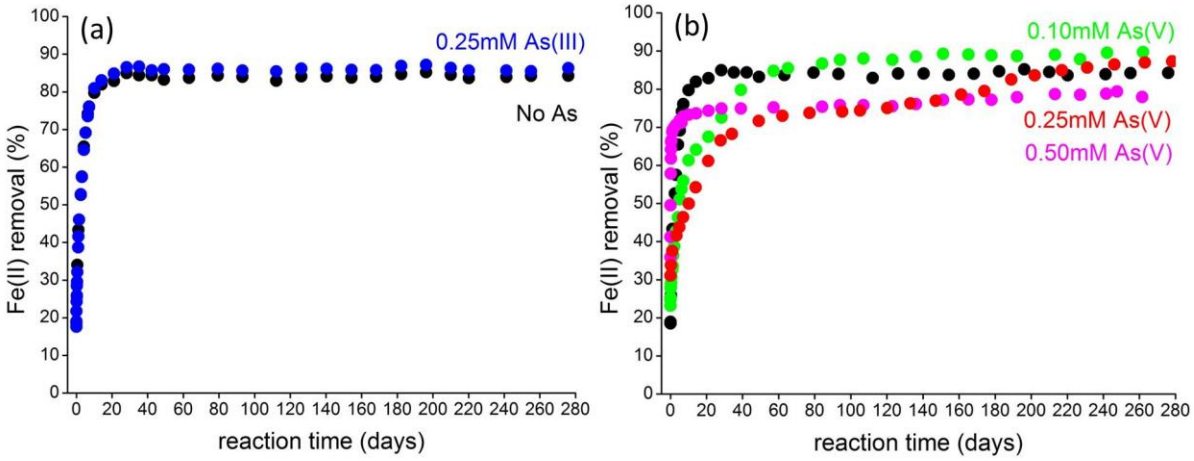

Figure 1. Kinetics of Fe(II) sorption in anoxic suspensions of 5.0 g L^{-1} γ-Al_2O_3 at pH 7.5 in single-sorbate and dual-sorbate experiments containing **(a)** As(III) and **(b)** As(V) at the concentrations indicated. The Fe(II) concentration was 1.0 mM in all systems.

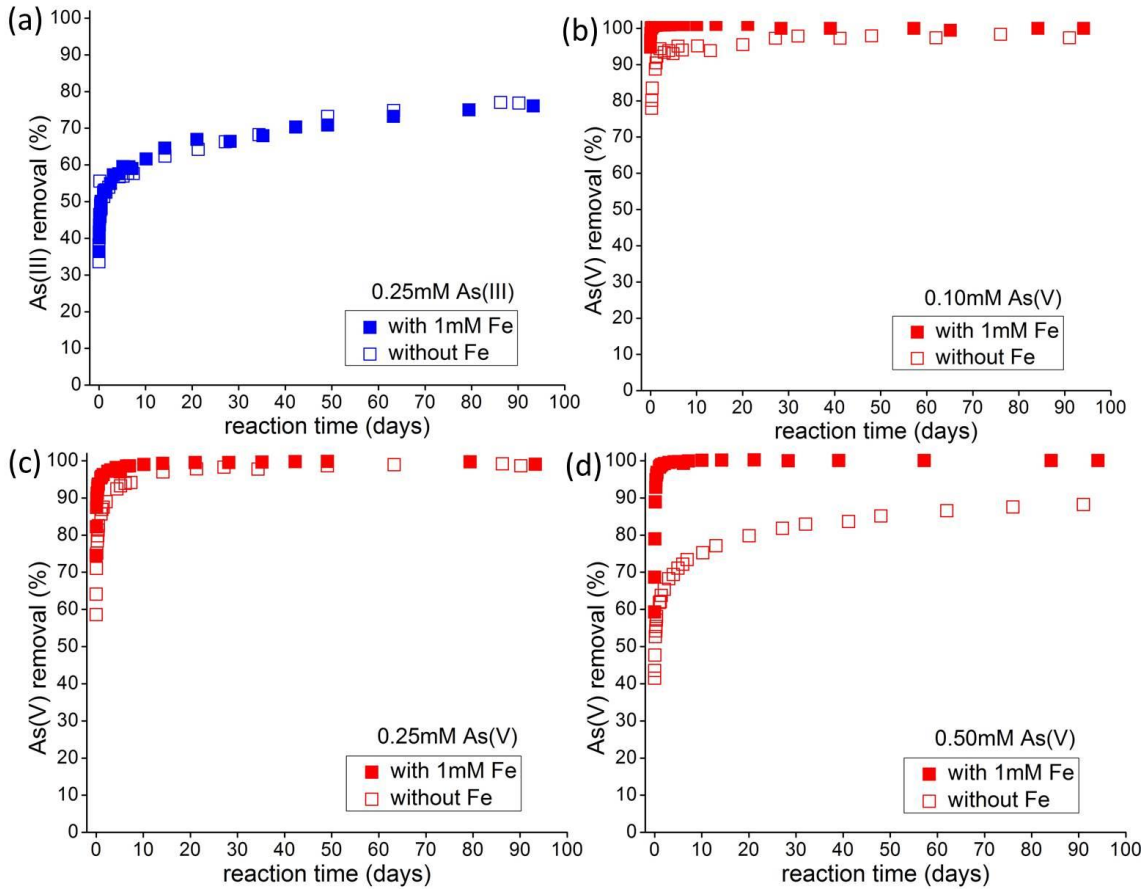

Figure 2. Kinetics of As sorption onto 5.0 g L^{-1} γ-Al_2O_3 at pH 7.5 in the presence and absence of 1.0 mM Fe(II), for **(a)** 0.25mM As(III); **(b)** 0.10 mM As(V); **(c)** 0.25 mM As(V); and **(d)** 0.50 mM As(V).

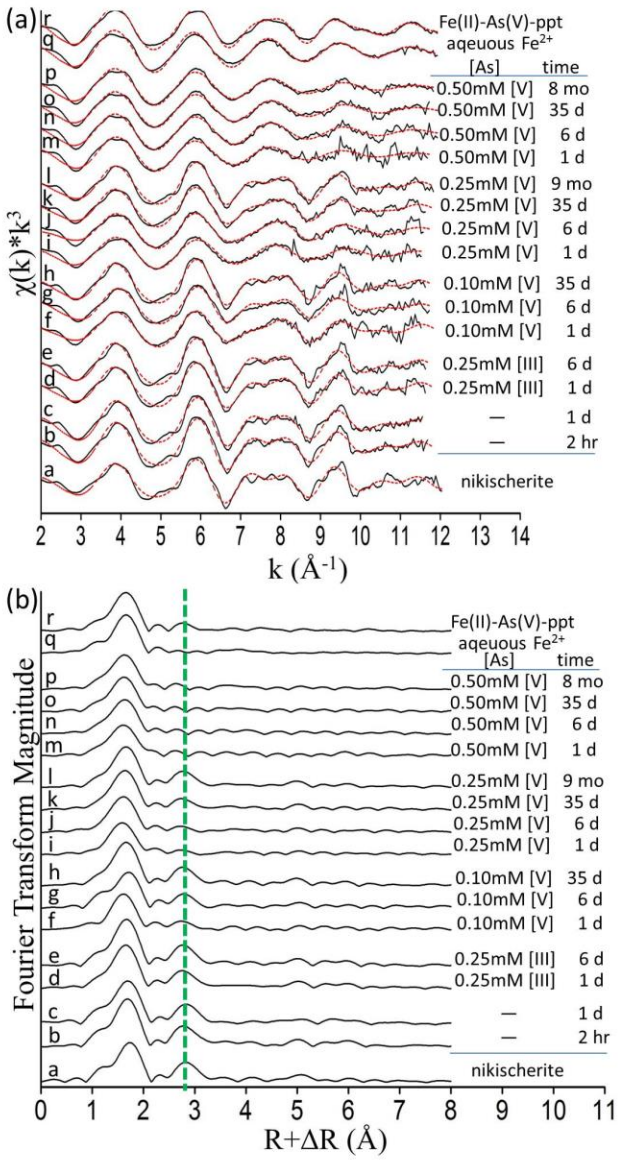

Figure 3. Fe *K*-edge EXAFS data of Fe references and sorption samples from single-sorbate and dual-sorbate systems containing 1.0 mM Fe(II), reacted at variable As(III) and As(V) concentrations for reaction times up to 9 months: **(a)** k^3-weighted χ spectra; and **(b)** corresponding radial structure functions (RSFs). Solid and red dotted lines in panel (a) represent raw and fitted spectra, respectively. Green vertical dashed line in panel (b) locates second-shell Fe-Fe/Al backscatters in the nikischerite and Fe(II) sorption samples, and second-shell Fe-Fe/As backscatter in Fe(II)-As(V) precipitate. The fit results are summarized in Table S1.

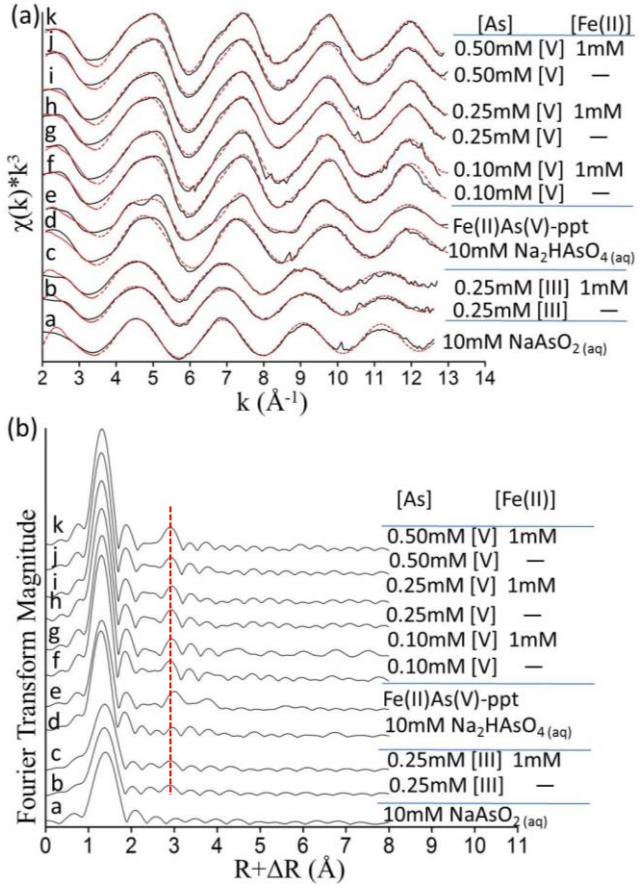

Figure 4. As *K*-edge EXAFS spectra of As reference and sorption samples from single-sorbate systems and dual-sorbate systems containing 1.0 mM Fe(II). The reaction time of the sorption samples was 6 days. **(a)** k^3-weighted χ spectra and **(b)** corresponding radial structure functions (RSFs). Solid and red dotted lines in panel (a) represent raw and fitted spectra, respectively. The red dotted line panel b locates second-shell Al neighbors in the As(V) and As(III) sorption samples. The fit results are summarized in Table S2.

TOC figure

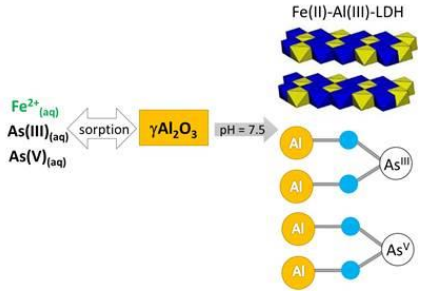
Fe(II)-Al(III)-LDH
$Fe^{2+}_{(aq)}$
$As(III)_{(aq)}$
$As(V)_{(aq)}$
sorption
γAl_2O_3
pH = 7.5
Al
Al
Al
Al
As^{III}
As^{V}